Spark Ignition of Turbulent Premixed and Non-premixed Opposed Jet Flames

S.F. Ahmed*
Engineering Department, University of Cambridge, Cambridge, CB2 1PZ, UK

R. Balachandran†
Mechanical Engineering, University College London, London, WC1E 7JE, UK

Y.-Y. He‡, and E. Mastorakos§
Engineering Department, University of Cambridge, Cambridge, CB2 1PZ, UK

The probabilistic nature of ignition of premixed and non-premixed turbulent opposed-jet flames has been examined and the flame structures following ignition have been visualized directly and with OH-PLIF. It has been found that high bulk velocities decrease the ignition probability in all locations and for all flames. Ignition is sometimes possible even in locations where there is negligible probability of finding flammable mixture and is sometimes impossible in locations with high probability of flammable fluid. The edge flame propagation speed is also estimated.

I. Introduction

Understanding spark-ignition of turbulent flames, especially non-premixed, is not yet at a point that quantitative theoretical predictions can be made, although ignition of non-premixed combustion is important in high-altitude relight of aviation gas turbines, in industrial furnaces, and in some GDI automotive engines. Experiments with spark ignition of jet diffusion flames[1,2] showed that the probability of the emergence of an initial flame kernel in the spark neighbourhood is approximately equal to the probability of finding air-fuel mixture within the flammability limits. This concept has been further explored to provide a quantitative explosion risk assessment[3] with CFD and a presumed shape of the PDF of the mixture fraction. Recently, this experiment has been re-visited[4] and it was shown that, if ignition is meant to imply the achievement of a full jet diffusion flame and not just the emergence of a small kernel that may be convected with the flow without causing flame ignition, the ignition probability is reduced and can be zero even in locations that have finite probability of flammable mixture fractions. The difference was attributed to local strain effects or high velocities that may not allow the flame kernel to grow or a flame to propagate, despite the local mixture fraction being flammable.

This paper presents additional measurements of ignition probability and of flame speed following ignition in a different flow to clarify further these issues. The opposed-jet geometry is chosen because it provides good control of the strain rate and good optical access. The experiments in this paper have been performed for both premixed and non-premixed flames for comparison. The local flow properties are shown to affect the success of ignition, and a new, non-local effect is demonstrated where the flame may ignite even if the spark is away from the flammable mixture.

II. Experimental Methods

The burner (Fig.1) comprises two straight pipes of inner diameter D=25mm, surrounded by co-flows of nitrogen of diameter D_0=50mm, following the counterflow burner of Refs. 5,6. The pipes are separated by a distance H=D for the experiments reported here. The upper pipe carries air, while the lower pipe carries methane, pure or premixed with air. The degree of premixing is described by the volume fraction of air, X, which is 80% for most of the

* PhD student, Engineering Department, University of Cambridge, Cambridge, CB2 1PZ, UK.
† Lecturer, Mechanical Engineering Department, University College London, London, WC1E 7JE, UK.
‡ Student, Engineering Department, University of Cambridge, Cambridge, CB2 1PZ, UK.
§ Reader, Engineering Department, University of Cambridge, CB2 1PZ, UK.Email: em257@eng.cam.ac.uk

experiments with non-premixed flames in this paper. Despite the high air premixedness, the flame is still non-premixed as the fuel requires additional air from the top stream to combust. The stoichiometric mixture fraction ξ_{st} is ξ_{st}=0.452, while the lean and rich flammability limits are ξ_{lean}=0.233 and ξ_{rich}=0.732 respectively.

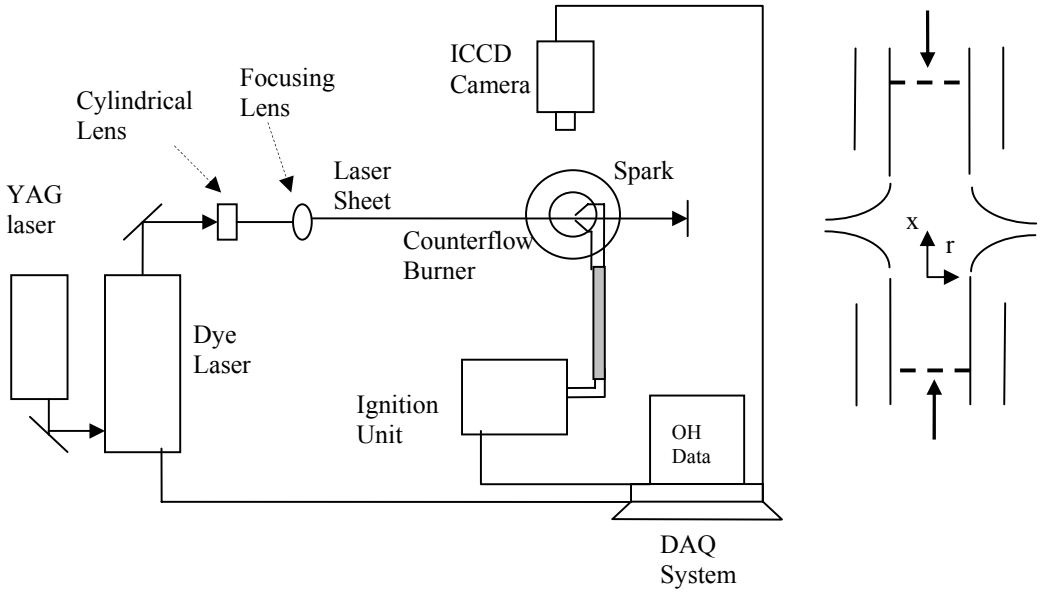

Figure 1. Schematic diagram of the test rig and the optical layout for PLIF imaging.

When the rich flammability limit is surpassed, then the lower stream contains a flammable mixture and its composition is described by the equivalence ratio, ϕ, with ϕ=0.8 only studied here. The bulk velocity of the upper jet (air) is U_b. To achieve a symmetric flow, the momentum flow rates of the two jets must be equal which implies that the velocity of the lighter (fuel) jet is higher than the velocity of the air jet, although the difference is very small for X=80% and the premixed flames since the density of the two streams are approximately equal. At a distance of 60 mm from the exits, perforated plates with 40% solidity and a hole size of 3 mm have been used to promote turbulence. Following Ref. 6, the turbulent fluctuations, u', and the integral lengthscale, L_t, at the exit of the nozzles are uniform across the pipe and approximately u'/U_b=10% and L_t=3 mm. For the present jet spacing, the axial velocity profile across the jets is approximately top-hat[6].

An ignition system was especially designed to produce repeatable sparks whose energy and duration could be varied independently. The main features of the unit can be found in Ref. 4 and followed the practice of Ref. 7. The spark was created between two stainless steel electrodes of 0.7 mm diameter, which were placed as shown in Fig.1 to ensure minimum disturbance to the flow field. The electrodes had pointed edges to reduce the heat loss from the spark and the distance between them was 2 mm. The two electrodes were attached to a twin-bore ceramic tube, which was traversed axially and radially to cover the whole flow field with 0.1 mm resolution. For the experiments described here, the spark had duration of 400 μs and the electrical energy delivered by the circuit was 100 mJ. For each position, 50 independent spark events were performed and the percentage of events resulting in a flame establishment (i.e. flame kernel growing with time and propagating across the stagnation plane) gave the ignition probability, P_{ign}.

The mixture fraction has been measured by Planar Laser Induced Fluorescence of acetone seeded in the fuel stream, to approximately 20% by volume. To excite the fluorescence, a fourth harmonic out of a Nd:YAG (Continuum Surelite) laser at 266 nm was used. The beam was spread into a vertical sheet with thickness of about 0.15 mm, by a combination of a 25-mm focal length cylindrical lens and a 500-mm focal length lens. The laser sheet passed through the centreline of the burner. The broadband PLIF signal was captured by an intensified CCD camera (LaVision). The images were subsequently corrected for background noise, non-uniformity in laser sheet intensity, and local intensity variation due to laser absorption. Following Ref. 8, Wiener filtering was performed to remove noise so that local mixture fraction gradients could be estimated to give the scalar dissipation rate in the two imaged dimensions.

PLIF of the OH radical has been used to examine the flame structure at various instants following the initial kernel generation. For the OH measurements, the output from a Nd:YAG laser was used to pump a Dye laser (Fig.1). The frequency doubled beam was tuned at 283.00 nm to excite the Q1(6) transition of A-X(1-0) band. The beam was spread into a vertical sheet with the same optical arrangement mentioned above for the acetone PLIF. The OH fluorescence from the (0,0) and (1,1) bands near 310 nm was captured by a Nikkor 50 mm lens and an ICCD camera fitted with a combination of Scott glass UG11 and WG305 filters[9].

The flame propagation was also monitored with a Phantom V4.2 Digital High Speed Camera fitted with a fast intensifier. A number of movies were captured with 4200 fps for successful and failed ignition events at different locations in the flow field in order to understand the behavior of the flame front from the moment of the spark until the establishment of the full planar turbulent flame.

III. Results and Discussion

A. Mixing Field

Figure 2 shows an instantaneous mixture fraction contour. It is evident that mixing occurs across a thin interface between the upper and lower streams that is about 1 mm thick, which seems to undulate due to the turbulence. It is also evident that mixing occurs between the jet and the co-flow, but these large radial locations are not of interest here, since we concentrate on the region up to about a pipe radius. It has also been found that the mean, variance, and the PDF shapes depend on axial distance only, at least for $r<D/2$. They do not depend on the jet velocity[6] and the PDF shape can be very well approximated by a beta-function shape[10].

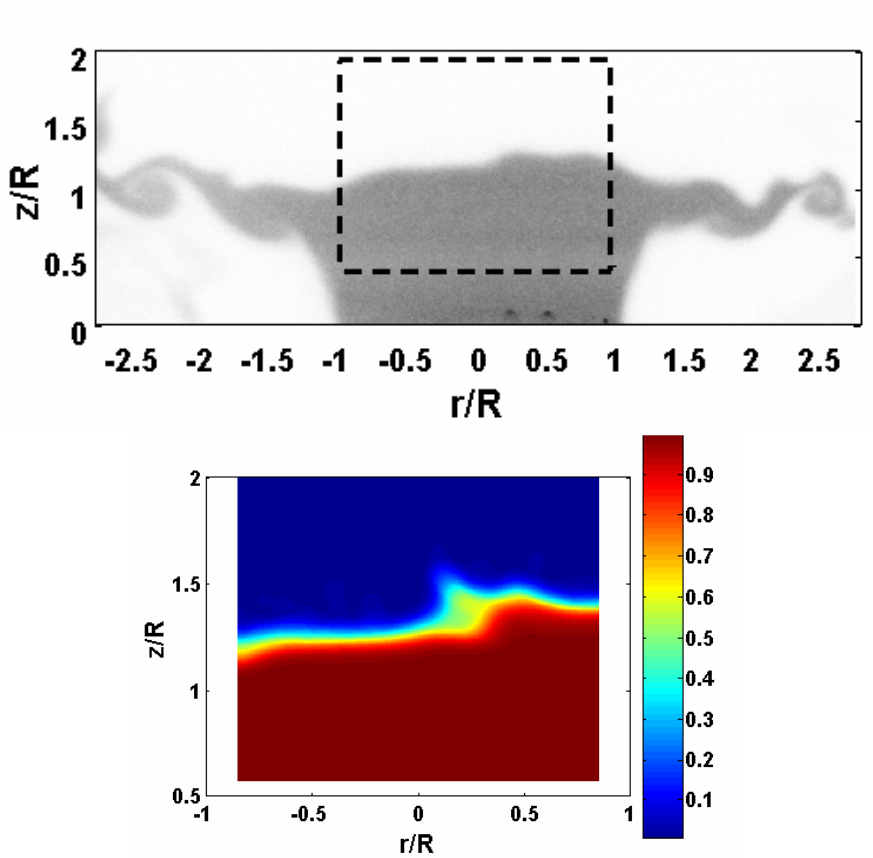

Figure 2. Typical instantaneous acetone PLIF image showing the region of interest and the corresponding mixture fraction image. From Ref. 10.

B. Flame Visualization and Structure

Following ignition at the spark, a thin flame starts to grow to fill the whole stagnation region (Fig. 3). In the case of the non-premixed flame, the flame propagates probably along the stoichiometric contour within the mixing layer. It is important to mention that the ignition event shown in Fig. 3 happened by using a single spark. Therefore the flame kernel is created around the spark area and then the flame starts propagating from this location. However, if a high frequency spark is used, the flame can be initiated *away* from the spark even if the probability of finding flammable composition there is zero. Figure 4 shows the emergence of a premixed flame in the fuel-air (lower) stream by continuous sparking at the air (upper) stream in which the spark is so far away from the stagnation plane that the probability of finding flammable mixture there is zero. This is attributed to the fact that the flow can convect the heat of the spark towards the stagnation region, where the chances of finding flammable mixture are finite. Hence, a flame may be initiated by a non-local spark. A similar effect has been observed in non-premixed flame ignition[10].

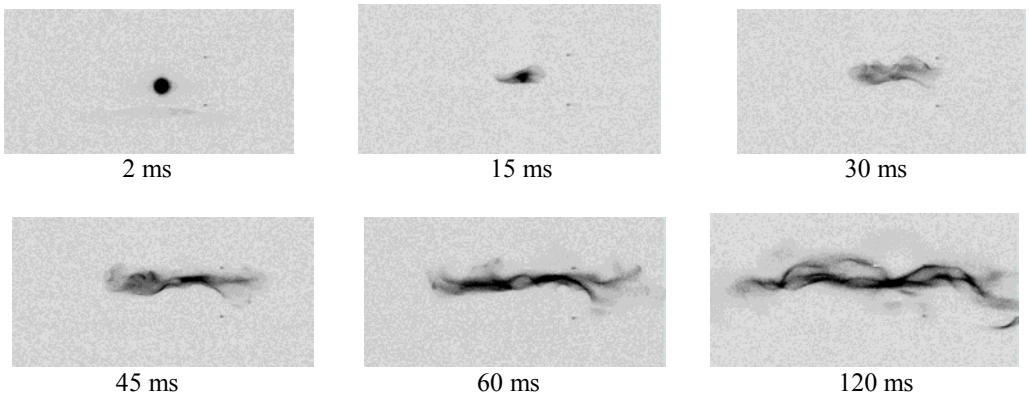

Figure 3. Instantaneous high-speed camera images of the non-premixed flame during propagation at different times after the ignition. Spark applied at the stagnation point (centre of the image). Fuel from below, air from above. U_b=2 m/s, X=80%. The images shown correspond to a region about 40 x 25 mm.

Figure 4. Instantaneous high-speed camera images at different instants following a 50 Hz spark in the air stream of an opposed-jet premixed flame. Air from above, air-fuel mixture at ϕ=0.8 from below. The images correspond to a region about 150 x 70 mm.

The OH-PLIF imaging of the ignition event shows that the flame leading edge during propagation is not a triple flame, whether a flame is premixed or non-premixed, but a so-called "edge flame"[11]. Figures 5 (a) and (b) show the structure of the flame during propagation for the premixed and non-premixed flame, respectively. Images such as those of Fig. 2 can be used to estimate the scalar dissipation, χ, by calculating the axial and radial gradients of the mixture fraction ($\chi=2D_{mol}(\nabla\xi)^2$) and, for the conditions of the flames in Fig. 2, the instantaneous scalar dissipation at stoichiometry is between 1 and 10 s^{-1}. For high scalar dissipations, the lean and rich branches of a triple flame may merge[12,13] consistent with the images in Fig. 5 that show a single reaction zone. Note also the thicker premixed flame, which is due to the fact that the flame is farther away from the stagnation plane than the non-premixed flame.

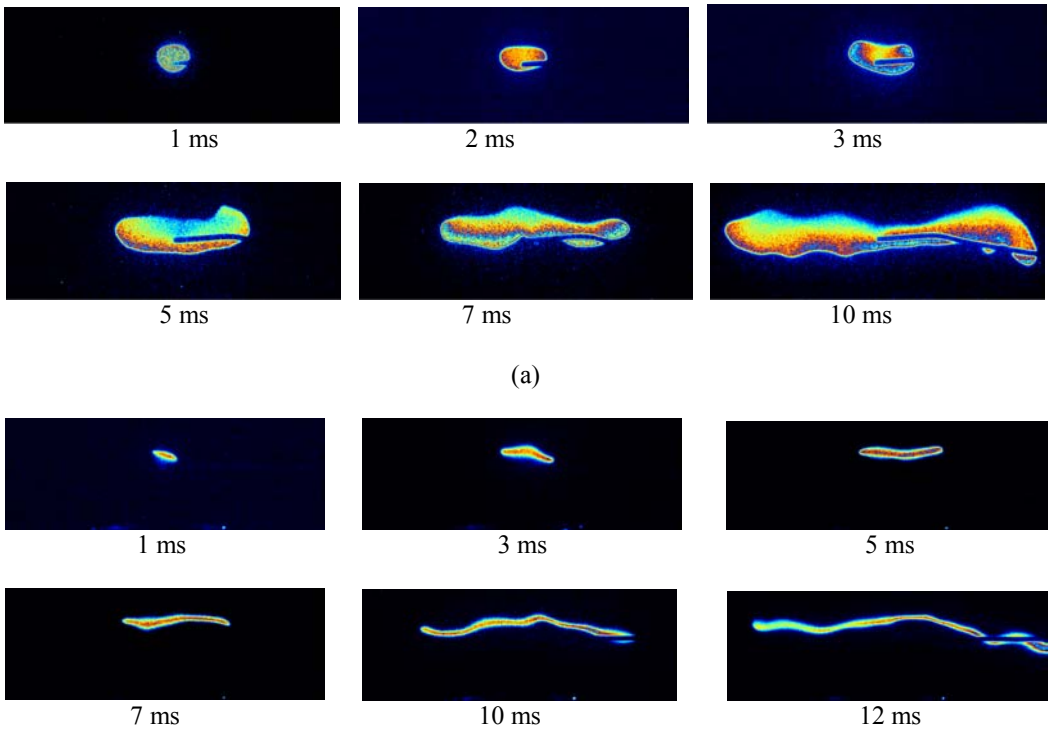

Figure 5. Instantaneous OH-PLIF mages of the flame during propagation at different times after the ignition. Spark applied at the stagnation point (centre of the image). Fuel from below, air from above. (a) Premixed flame, U_b=2 m/s, ϕ=0.8; (b) Non-premixed flame, U_b=2 m/s, X=80%. The images shown correspond to a region about 40 x 25 mm. Images (b) are taken from Ref. 10.

C. Premixed Flame Ignition

Figure 6 shows contours of ignition probability, P_{ign}, for premixed flames for the same equivalence ratio but two values of the bulk velocity. Despite the fact that both contours have the same equivalence ratio spatial distribution, the ignition region clearly shrinks with the increase in velocity. Ignition is not possible for any radial location larger than r=15mm at U_b=2 m/s, while ignition with about 20% probability can be observed up to r=18mm at U_b= 1.5 m/s. This is possibly due to the fact that the flow velocity there is high and hence the flame cannot expand against the radially-flowing fluid and also due to the dilution with the opposing air. However, ignition is always possible well into the fuel-air stream (i.e. at low z and r). Figure 6 also shows that above z = 17 mm in the axial direction there is no ignition and that P_{ign} decreases from 100% to zero across a region of thickness around 6mm in the low velocity case and 10mm in the high velocity case. Overall, there is a significant reduction in the ignition probability values between the two cases. Since the equivalence ratio field and its fluctuations are not expected to be different with an increase in velocity, the change in ignition probability suggests that the flow plays a role. In particular, we attribute the reduction in ignition probability to the detrimental effect of local high turbulence on the success of ignition regardless of the existence of flammable mixture at the location of the spark. Similar behavior has been observed before with the ignition of turbulent jets[4] and will be described next for opposed-jet non-premixed flames.

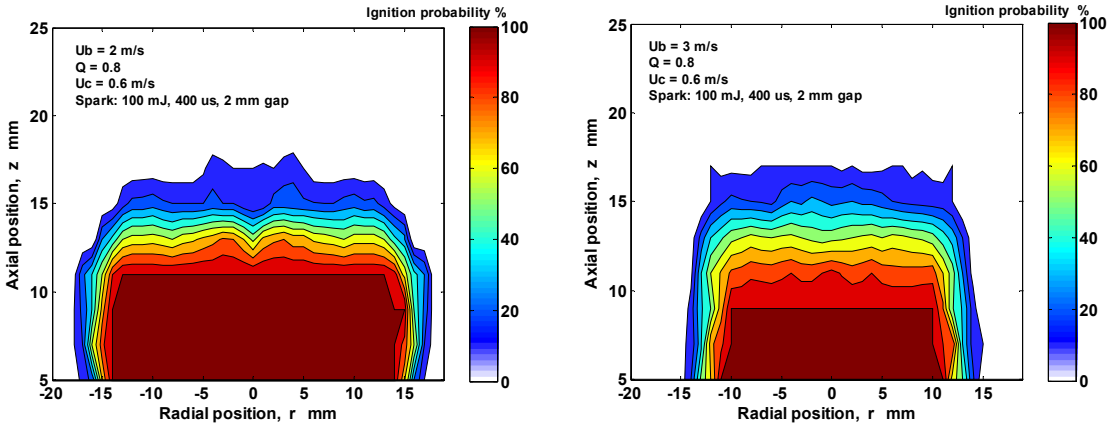

(a) (b)

Figure 6. Ignition probability contour for premixed flames with (a) U_b=1.5 m/s, ϕ=0.8; (b) U_b=2 m/s, ϕ=0.8.

D. Non-premixed Flame Ignition

Figure 7, taken from Ref. 10 and included here for completeness in comparing with the premixed flame, shows contours of ignition probability, P_{ign}, for non-premixed flames. The ignition probability decreases as the velocity increases and it becomes zero at r>12mm. Also, finite probability is found far from the stagnation region along the centreline where the mixture fraction fluctuations are essentially zero and the fluid is beyond the flammability limits. It is also interesting to note from Fig. 7 that the shape of the contour is different from the contour of the premixed flame (Fig. 6) and also different from shape of the probability of finding flammable mixture, which is uniform in the radial direction because the mixture fraction PDF is uniform with radius[10]. The fact that ignition can occur even at locations where the PDF of finding flammable material is nominally zero can be explained partly by the non-local effect visualised in Fig. 4 and partly by the fact that the initial spark kernel can become a few mm in size[4], which hence increases the chances of hot fluid touching flammable mixtures. The finding that P_{ign} can become zero in locations where there is finite probability of flammable mixture fractions is probably due to the fact that, as the radial velocity increases with radius, after a certain radius the edge flame speed is not greater than the local flow velocity to allow the flame to spread. Finally, an increase in U_b does not alter the mixing field, but it decreases the ignition probability, which implies that high local velocities are detrimental to ignition despite the presence of flammable mixtures. This is fully consistent with the observation in Fig. 6 for the premixed flame. For a more detailed discussion of these points, for a direct comparison of the ignition probability with the probability of finding flammable mixture, and for additional data for other X, see Ref. 10.

E. Ignitability limits

In another experiment, the maximum velocity that the flame can be ignited has been measured for the premixed and non-premixed conditions and compared to the extinction velocity of the same flame. Figure 8 shows that both velocities increase with X, peak at the stroichiometric mixture, and decrease towards very lean premixed flames. For all flames, it is not possible to ignite the flame if the bulk velocity exceeds 90% of the extinction velocity. The fact that the maximum velocity for ignition is smaller than the extinction velocity is in full agreement with the theoretical study of Ref. 14, which predicts that the maximum strain rate that a steady laminar flame edge can sustain is less than the extinction strain rate of the corresponding premixed or non-premixed flame. This was related to the fact that the edge flame during propagation is subjected to a higher heat flux away from the reaction zone in the radial direction ahead of the flame front, which results in excessive reduction in the flame front temperature and then flame extinction[14]. The data suggests that, even if the operating conditions are those of stable combustion, ignition of the flame may not be possible. Laminar flame calculations[15] showed that ignition may not be feasible even at a strain rate as low as 50% of the extinction value, which is consistent with the present observation and also with typical gas turbine ignition data[16] that show an ignition loop narrower than an extinction loop.

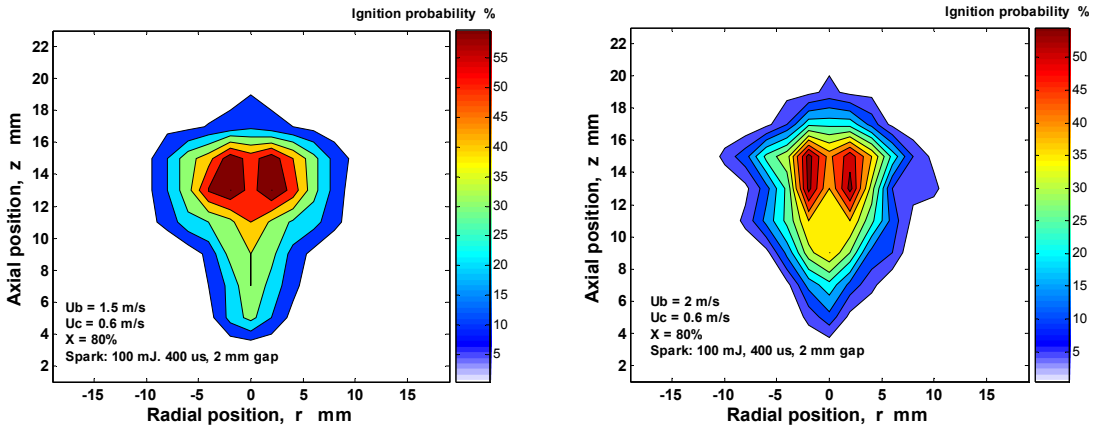

(a) (b)

Figure 7. Ignition probability contour for non-premixed flame with (a) U_b=1.5 m/s, X=80%; (b) U_b=2 m/s, X=80%. Reproduced from Ref. 10.

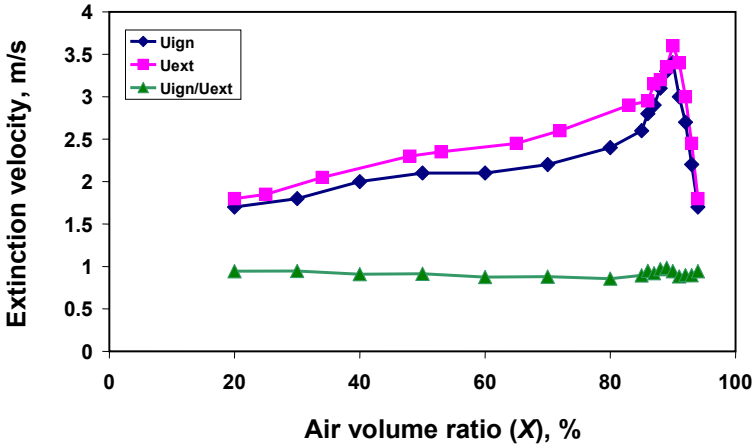

Figure 8. The extinction velocity, the maximum possible velocity for ignition, and their ratio as a function of air volume ratio of the fuel stream. The flame is deemed premixed for X>85%. The peak extinction velocity corresponds to a stoichiometric mixture in the lower jet.

F. Edge Flame Speed

Following ignition, images such as those of Fig. 5 have been used to measure the radial position of the flame edge as a function of time, when the flame is ignited at the centreline. Then, the average position over approximately 100 images has been measured and plotted versus time from the spark. It should be mentioned that the scatter plot of the radial position of the edge flame from these images shows that the flame is propagating within a region of about 10 mm thick, with the axial fluctuation probably related to the flapping of the instantaneous stoichiometric iso-surface across the mixing layer[10]. Figure 9 shows that the speed of edge flame propagation (i.e. slope of the curve) is greater for the high U_b flow and slightly decreases at large times from ignition (i.e. at large radii). Figure 9 also shows that the premixed flame propagation speed is higher than that of the non-premixed flame at the same U_b. Using the data up to r=15mm, the propagation speed (averaged over all radii) is about 2.4 m/s for the premixed flame at U_b = 2m/s, while it is about 1.7 m/s for U_b = 2m/s and about 1.4 m/s for U_b = 1.5 m/s in the non-premixed flame.

In these experiments, the flame is ignited on the centreline and hence the radial velocity assists flame spreading. The mean radial velocity is estimated as V=2$U_b r/H$ and this has been subtracted from the measured average edge flame propagation speed as a function of radius, estimated from Fig. 9a by calculating the derivative. The result is an

estimate of the relative edge flame propagation speed (i.e. speed relative to the flow) and this is shown in Fig. 9b. It is evident that after about 5 mm from the centreline, the net speed is approximately constant at about 0.6 m/s for the premixed flame and about 0.3 m/s for the non-premixed flame. The latter is slightly lower than the laminar burning velocity, S_L, of a stoichiometric methane air premixed flame (0.4m/s), while the former is about twice the S_L of a mixture of ϕ=0.8. More detailed measurements would of course necessitate a detailed measurement of the flow velocity ahead of the flame.

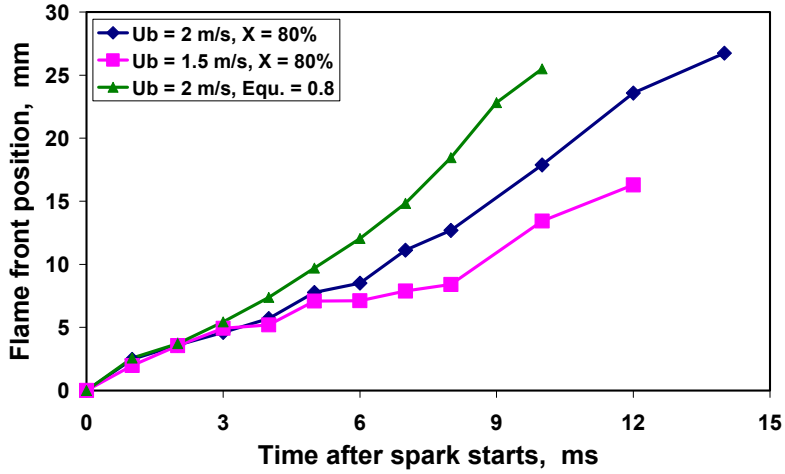

(a)

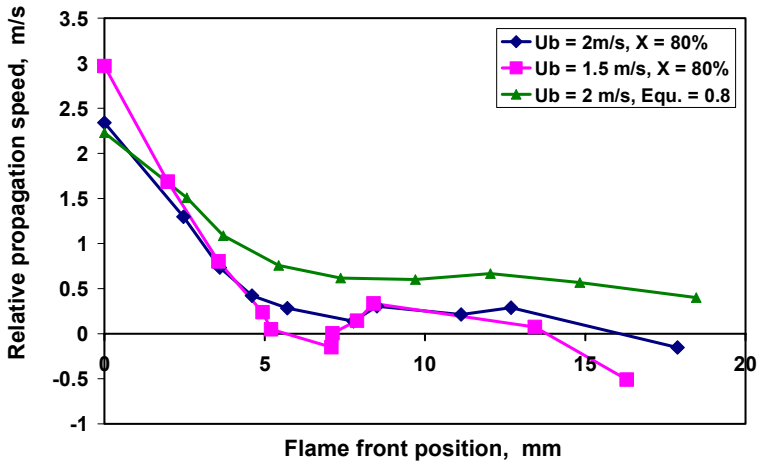

(b)

Figure 9. (a) Average flame position *vs.* time from spark for premixed and non-premixed flames. (b) Estimated relative flame speed *vs.* radial position from spark.

IV. Conclusion

The success of igniting planar premixed and non-premixed turbulent opposed-jet flames of methane with a spark has been quantified by measuring the ignition probability for various bulk strain rates and fuel premixing with air. PLIF of OH has also been used to visualise the flame following ignition. The main conclusions from the present work are the following. Firstly, with an increase in the bulk velocity the ignitable region shrinks and the ignition probability decreases for both premixed and non-premixed flames. Secondly, ignition can be achieved from a spark far away from the region where flammable region exists with finite probability, again for both types of flames. This is attributed to the mean convection that carries the gases heated by the spark towards the flammable air-fuel region. Thirdly, the probability of ignition becomes zero at large radii, possibly because the flame kernel at large radii experiences large adverse radial velocities and hence cannot expand and because the dilution with co-flowing and opposing air leans out the mixture. Finally, the non-premixed flame expands as an edge flame, with no evidence of triple flame structure, probably due to the large scalar dissipation rates experienced. The edge flame speed relative to the laboratory coordinates increases with U_b, while the estimated edge flame speed relative to the radial flow is higher than S_L for the premixed flame and is less than S_L for most of the radial travel of the non-premixed flame as it expands to fill the stagnation plane. The data are suggested as a suitable test bed for validating advanced modelling approaches for ignition and flame propagation in the context of RANS and LES.

Acknowledgments

This work has been supported by the Department of Trade and Industry, U.K. and Rolls-Royce plc. We thank Dr. N. Chakraborty of Liverpool University and Mr. E.S. Richardson of CUED for useful discussions. S F Ahmed wishes to thank BP Egypt for a fellowship to study for a PhD at Cambridge University.

References

[1]Birch, A. D., Brown, D. R., and Dodson, M. G., *Proc. Combust. Inst.,* Vol. 18, 1981, pp. 1775-1780.
[2]Birch, A. D., Smith, M. T. E., Brown, D. R., and Fairweather, M., *Proc. Combust. Inst.*, Vol. 21, 1986, pp. 1403-1408.
[3]Alvani, R. F., and Fairweather, M., In *Turbulence, Heat and Mass Transfer*, Vol. 4, 2003, Hanjalic et al. (Eds), pp. 911-918.
[4]Ahmed, S.F., and Mastorakos, E., *Combust. Flame*, 2006 (To be published)
[5]Mastorakos, E., Taylor, A. M. K. P., and Whitelaw, J. H., *Combust. Flame*, Vol. 91, 1992, pp. 40-54.
[6]Mastorakos, E., "Turbulent combustion in opposed jet flows", PhD Dissertation, Imperial College, London, 1993.
[7]Dreizler, A., Kaminski, C.F., Hult, J., Alden, M., Lindenmaier, S., Mass, U., and Baum, M., *Proc. Combust. Inst.,* Vol. 28, 2000, pp. 399-405.
[8]Markides, C. and Mastorakos, E., *Chem. Eng. Sci.*, Vol. 61, 2006, pp. 2835-2842.
[9]Balachandran, R., "Experimental investigation of the response of turbulent premixed flames to acoustic oscillation," PhD Dissertation, University of Cambridge, Cambridge, 2005.
[10]Ahmed. S.F., Balachandran, R., and Mastorakos, E., *Proc. Combust. Inst.*, Vol. 31, 2006 (To be published).
[11]Buckmaster, J., *Prog. Energ. Conbust. Sci.*, Vol. 28, 2002, pp. 435-475.
[12]Carnell Jr., W.F., and Renfro, M.W., *Combust. Flame*, Vol. 141, 2005, pp. 350-359.
[13]Favier, V., and Vervisch, L., *Combust. Flame*, Vol. 125, 2001, pp. 788-803.
[14]Vedrajan, T.G. and Buckmaster, J., *Combust. Flame*, Vol. 114, 1998, pp. 267-273.
[15]Richardson, E.S., and Mastorakos, E. *Combust. Sci. Tech.*, 2006 (To be published).
[16]Lefebvre, A. H., "Gas turbine combustion," Taylor and Francis, London, 1998.